

# Atroposelective interrupted CuAAC reaction using cyclic diaryliodoniums

Received: 22 March 2025

Accepted: 31 October 2025

Published online: 24 January 2026

Check for updates

Yuanyuan Li<sup>1</sup>, Shan Yang<sup>1</sup>, Longhui Duan<sup>1</sup> & Zhenhua Gu<sup>1,2</sup>✉

Copper-catalyzed azide–alkyne cycloaddition (CuAAC) is a pivotal strategy for joining two fragments, including bioactive moieties under mild conditions. In recent years, “interrupted” CuAAC reaction has emerged by intercepting copper triazolide intermediates, thereby significantly broadening the scope of these transformations. However, asymmetric transformations based on the interruption of copper triazolide intermediates have remained elusive. In this work, we present an efficient and mild approach that intercepts a copper triazolide intermediate with a cyclic diaryliodonium reagent, enabling a three-component coupling of the cyclic diaryliodonium species, an alkyne, and an azide under atroposelective control. This method constitutes an asymmetric interrupted CuAAC reaction and furnishes a diverse array of structurally unique atropisomeric biaryl triazoles. Mechanistic investigations reveal an unusual secondary kinetic isotope effect for the terminal alkyne, while in situ calorimetry–based reaction progress kinetic analysis identifies the individual reaction orders of each substrate: formal 0.4th-order for cyclic diaryliodonium and first-order for both the alkyne and the azide. The overall rate is governed by copper-mediated cyclometallation of the alkyne and azide, as well as the oxidative addition of the copper triazolide intermediate to the cyclic diaryliodonium reagent.

Since the independent development of copper-catalyzed azide–alkyne cycloaddition (CuAAC) reaction by Sharpless<sup>1</sup> and Meldal<sup>2</sup> groups, CuAAC reaction has been widely used in organic synthesis, materials science, bioconjugation and chemical biology (Fig. 1a)<sup>3–9</sup>. The discovery of copper as a catalyst offers two key advantages: (a) The copper catalyzed reaction yields highly regioselective 1,4-triazoles, and lowers the reaction temperature compared to the classic Huisgen cycloaddition between azide and alkyne (e.g., reflux in toluene), thereby enabling applications in biochemistry; (b) The mechanistic studies have confirmed the existence of a key metalocycle intermediate<sup>10</sup>, the 1,4-substituted triazolyl copper species **M1**, which have ever been unambiguously characterized by X-ray single crystal analysis<sup>11,12</sup>. Building on these findings, a range of interrupted reactions have been developed (Fig. 1a). After the pioneer work of Wu et al.<sup>13</sup>, a variety of electrophiles, such as allyl halide<sup>14</sup>, RS(O)<sub>2</sub>SR<sup>15</sup>,

acid chloride<sup>16</sup>, CuI/*N*-bromosuccinimide<sup>17</sup>, *SS*-tert-butyl *p*-toluenesulfonyl(dithioperoxyate)<sup>18</sup>, Bu<sub>3</sub>SnOMe<sup>19</sup>, diselane<sup>20</sup>, and nitrene<sup>21</sup> etc.<sup>22–26</sup>, can be used to terminate the triazolyl copper species, a process typically referred to as the interrupted CuAAC reaction. Alternatively, less reactive species, i.e., sp<sup>2</sup>-hybridized aryl bromides and iodides<sup>27–30</sup>, can serve as terminating agents when utilized as intramolecular components to access cyclic 5-aryl-1,4-triazoles.

Motivated by wide applications of atropisomers (particularly axially chiral biaryl compounds)<sup>31–48</sup>, we have recently developed a copper-catalyzed highly stereoselective ring-opening reaction of cyclic diaryliodoniums to construct tetra-substituted biaryl atropisomers<sup>49,50</sup>. The retained C–I bonds in the product can be used for late-stage diversification<sup>51</sup>. This reaction is believed proceed through an oxidative addition of Cu(I) with cyclic diaryliodoniums to form Cu(III) intermediate **M2**, followed by reductive elimination to achieve the formation of

<sup>1</sup>Department of Chemistry, University of Science and Technology of China, Hefei, Anhui, PR China. <sup>2</sup>State Key Laboratory of Coordination Chemistry, Nanjing University, Nanjing, PR China. ✉e-mail: [zhgu@ustc.edu.cn](mailto:zhgu@ustc.edu.cn)

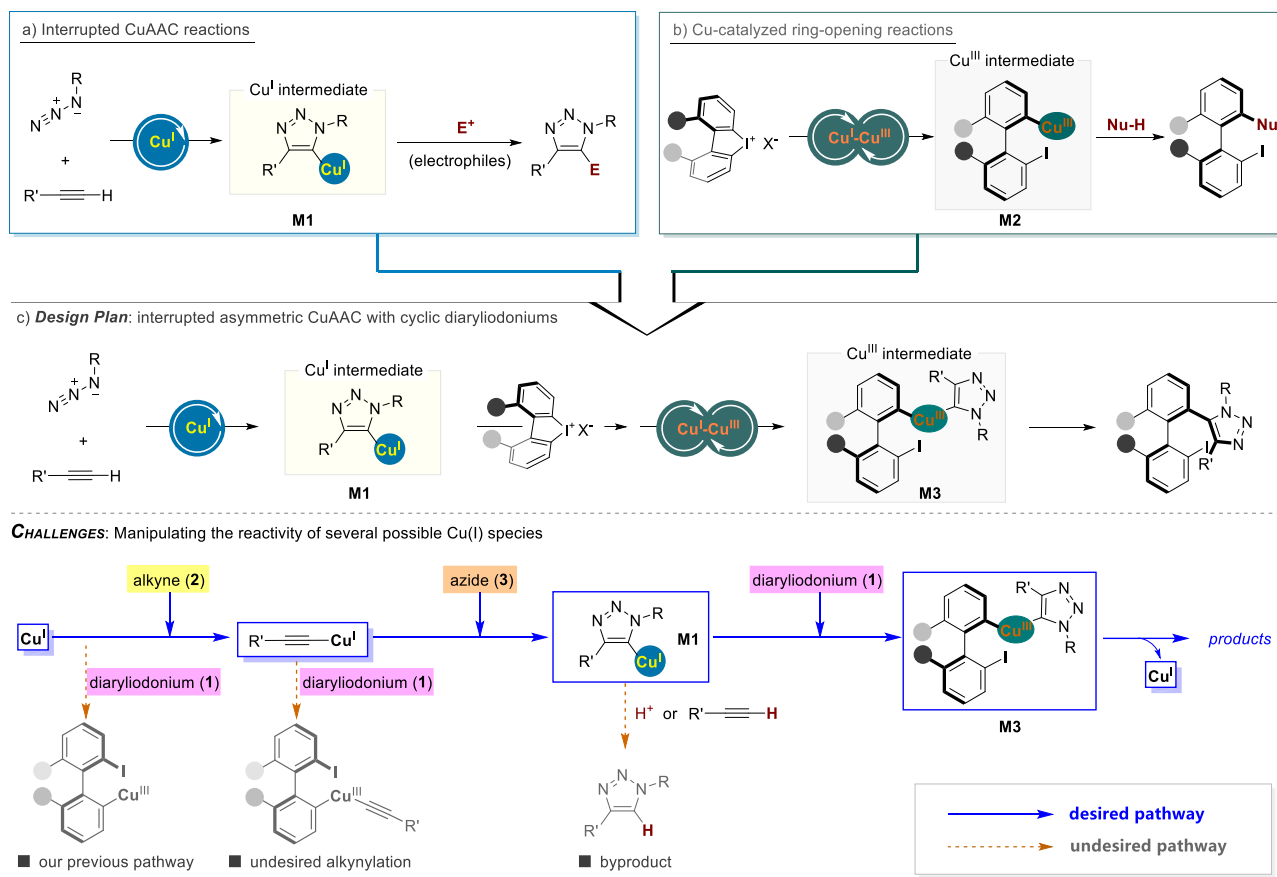


**Fig. 1** CuAAC reaction and Cu-catalyzed coupling of cyclic diaryliodoniums. **a** Interrupted CuAAC reaction. **b** Cu-catalyzed asymmetric ring-opening reaction of cyclic diaryliodoniums. **c** Our design plan: atroposelective interrupted CuAAC with cyclic diaryliodoniums.

carbon-heteroatom bonds (Fig. 1b). However, to date, apart from palladium-catalyzed carbonylation reactions by Hayashi<sup>52</sup>, Wu and Liao<sup>53</sup>, only heteroatom nucleophiles have been successfully applicable to this Cu-catalyzed asymmetric ring-opening reaction<sup>54</sup>.

In this work, we combine these two catalytic cycles, Cu(I)-Cu(I) cycle and Cu(I)-Cu(III) cycle, to realize an enantioselective diaryliodonium-interrupted CuAAC reaction, allowing for the participation of a formal carbon nucleophile in Cu-catalyzed ring-opening of cyclic diaryliodoniums (Fig. 1c). In addition to the significant challenge of controlling the enantioselectivity, careful management of competing side-reaction pathways is essential. For instance, three Cu(I) species,  $L^*Cu(I)$ ,  $RC\equiv CCu(I)$ , triazolyl copper(I) **M1**, might compete in the oxidative addition reaction with cyclic diaryliodonium, leading to the formation of three distinct Cu(III) intermediates. We hypothesize that the  $sp^2$ -hybridized carbon-copper **M1** is more electron-rich than either  $L^*Cu(I)$  or the  $sp$ -hybridized carbon copper  $RC\equiv CCu(I)$ , suggesting that **M1** may exhibit a higher oxidative tendency toward diaryliodoniums than the other two copper species. Moreover, in aprotic solvent, the final protonation of CuAAC intermediate **M1** is usually a slow process, and generally regarded as the rate-determining step<sup>55</sup>, providing an opportunity to trap this intermediate by diaryliodoniums, rather than through a slow protonation with terminal alkynes.

## Results and discussion

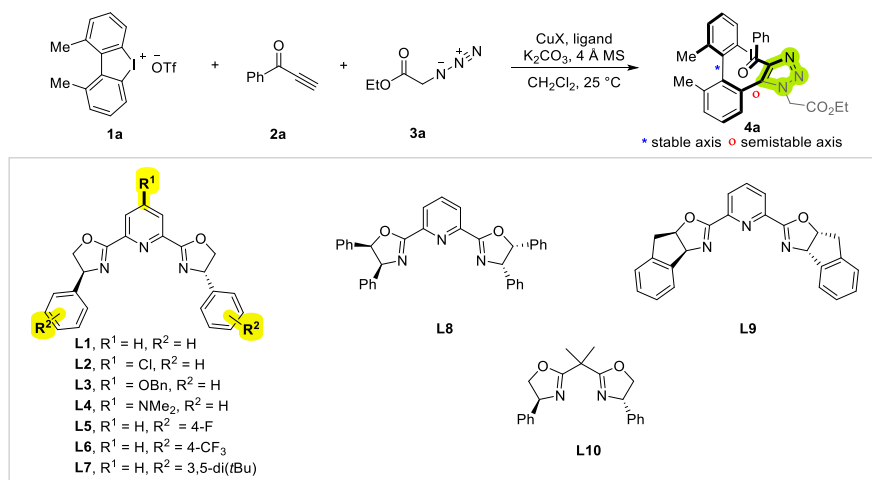
### Optimize the reaction conditions

In light of these considerations, we first selected functionalized alkyne **2a** and azide **3a** as substrates. Copper(II) triflate [ $Cu(OTf)_2$ ] was ineffective, despite the usual expectation that Cu(II) can undergo disproportionation to generate Cu(I) and Cu(III) or reduction to Cu(I) species via alkyne homocoupling (Table 1, entry

1)<sup>56</sup>. In contrast, the  $Cu(MeCN)_4PF_6/L1$  catalytic system successfully catalyzed the reaction, giving a moderate yield of **4a** with good enantioselectivity (entry 2). Product **4a** contains two potential chiral axes. Nuclear magnetic resonance ( $^1H$  NMR) analysis shows a diastereomeric ratio (dr) of -15:1, which varies with deuterium solvent choice (e.g.,  $CDCl_3$ ,  $CD_2Cl_2$ ,  $DMSO-d_6$ , toluene- $d_8$ ; see the Supplementary Fig. S1). These observations indicate that the phenyl-phenyl axis is stable, whereas the phenyl-triazole axis is semi-stable, undergoing rotation at room temperature. Reducing the reaction concentration improved the yield but slightly lowered enantioselectivity (entry 3). Increasing the proportion of **2a** and **3a** relative to **1a** provided no further yield improvement and instead diminished enantioselectivity (entry 4). Changing bases and modifying the electronic nature of the pyridinyl substituents in pyridine-2,6-bis(oxazoline) PyBox (**L2-L4**) did not provide better results (entries 5–9). We subsequently varied the amino-alcohol backbone and its electronic properties (**L5-L9**), but none yielded improved outcomes (entries 10–14). Notably, bis(oxazoline) ligand **L10** showed worse performance than pyridine-2,6-bis(oxazoline) ligand **L1** (compare entry 15 with entry 3). In addition, using  $K_2CO_3$  flame-dried under vacuum in a Schlenk tube further improved the reaction and exhibited good reproducibility (entry 16). The absence of 4 Å molecular sieves resulted in an improved yield, but a considerable drop in enantioselectivity (entry 17).

### Substrate scope

Upon identifying the optimal reaction conditions, we examined the scope of the reaction (Figs. 2 and 3). First, we focused on the influence of various substituents on arylalkynyl ketones. Overall, most *para*-substituents on phenylalkynyl ketones had minimal impact on yield or

**Table 1 | Reaction condition optimization<sup>a</sup>**

Entry	Cooper catalyst	Ligand	Base	4a	
				Yield/%	ee/%
1 <sup>b</sup>	Cu(OTf) <sub>2</sub>	<b>L1</b>	K <sub>2</sub> CO <sub>3</sub>	/	/
2 <sup>b</sup>	Cu(MeCN) <sub>4</sub> PF <sub>6</sub>	<b>L1</b>	K <sub>2</sub> CO <sub>3</sub>	66	90
3	Cu(MeCN) <sub>4</sub> PF <sub>6</sub>	<b>L1</b>	K <sub>2</sub> CO <sub>3</sub>	91	88
4 <sup>c</sup>	Cu(MeCN) <sub>4</sub> PF <sub>6</sub>	<b>L1</b>	K <sub>2</sub> CO <sub>3</sub>	90	82
5	Cu(MeCN) <sub>4</sub> PF <sub>6</sub>	<b>L1</b>	Na <sub>2</sub> CO <sub>3</sub>	71	90
6	Cu(MeCN) <sub>4</sub> PF <sub>6</sub>	<b>L1</b>	K <sub>3</sub> PO <sub>4</sub>	94	86
7	Cu(MeCN) <sub>4</sub> PF <sub>6</sub>	<b>L2</b>	K <sub>2</sub> CO <sub>3</sub>	91	88
8	Cu(MeCN) <sub>4</sub> PF <sub>6</sub>	<b>L3</b>	K <sub>2</sub> CO <sub>3</sub>	72	84
9	Cu(MeCN) <sub>4</sub> PF <sub>6</sub>	<b>L4</b>	K <sub>2</sub> CO <sub>3</sub>	13	81
10	Cu(MeCN) <sub>4</sub> PF <sub>6</sub>	<b>L5</b>	K <sub>2</sub> CO <sub>3</sub>	85	82
11	Cu(MeCN) <sub>4</sub> PF <sub>6</sub>	<b>L6</b>	K <sub>2</sub> CO <sub>3</sub>	89	68
12	Cu(MeCN) <sub>4</sub> PF <sub>6</sub>	<b>L7</b>	K <sub>2</sub> CO <sub>3</sub>	36	84
13	Cu(MeCN) <sub>4</sub> PF <sub>6</sub>	<b>L8</b>	K <sub>2</sub> CO <sub>3</sub>	37	18
14	Cu(MeCN) <sub>4</sub> PF <sub>6</sub>	<b>L9</b>	K <sub>2</sub> CO <sub>3</sub>	85	16
15	Cu(MeCN) <sub>4</sub> PF <sub>6</sub>	<b>L10</b>	K <sub>2</sub> CO <sub>3</sub>	6	7
16 <sup>d</sup>	Cu(MeCN) <sub>4</sub> PF <sub>6</sub>	<b>L1</b>	K <sub>2</sub> CO <sub>3</sub>	90	90
17 <sup>e</sup>	Cu(MeCN) <sub>4</sub> PF <sub>6</sub>	<b>L1</b>	K <sub>2</sub> CO <sub>3</sub>	97	44

Bold numbers correspond to ligand designations.

<sup>a</sup>Conditions: **1a** (0.1 mmol), **2a** (0.12 mmol), **3a** (0.12 mmol), [Cu] (0.010 mmol), ligand (0.02 mmol), 4 Å molecular sieves (80 mg), base (3.0 equiv) in CH<sub>2</sub>Cl<sub>2</sub> (4 mL), and stirred at 25 °C for 36 h. Isolated yields are reported, and ee values were determined by chiral stationary HPLC.

<sup>b</sup>2 mL of CH<sub>2</sub>Cl<sub>2</sub> was used.

<sup>c</sup>**2a** (0.20 mmol), **3a** (0.20 mmol) were used.

<sup>d</sup>K<sub>2</sub>CO<sub>3</sub> was flame dried under vacuum in a Schlenk tube.

<sup>e</sup>Without 4 Å molecular sieves in CH<sub>2</sub>Cl<sub>2</sub> (4 mL) and stirred at 25 °C for 3 h.

enantioselectivity (**4a–4i**), except for the nitro substituent, which led to a decreased enantioselectivity (83% ee) (**4j**). The structure and absolute configuration of compound **4j** (CCDC 2421103, see the Supplementary Table S3) were confirmed by single-crystal X-ray diffraction study. Large *meta*-substituents enhanced enantioselectivity (e.g., **4o**) but often reduced the yield; similarly, a 3,4-dimethoxy substituent offered a low yield of **4r**. Heteroaryl derivatives, such as those bearing 3-thiophene and 3-methyl-2-benzofuryl moieties, also reacted smoothly to afford the desired products. In general, *ortho*-substituents diminished the efficiency of this interrupted CuAAC reaction, resulting in somewhat reduced yields (**4v–4z**). 1-Alkyl-2-propyn-1-one derivative showed a slight drop in enantioselectivity (**4aa**), while the reaction with *N*-tolyl propargyl amide gave an even lower enantioselectivity of 76% ee (**5**). To explore the reaction compatibility of different substituted alkynes and azides, we conducted automated substrate screening using a chemical robot and identified suitable candidates for

this three-component cross-coupling reaction (Supplementary Table S1). When 2-(prop-2-yn-1-yl)isoindoline-1,3-dione was employed as a substrate, the reaction afforded the product (**6**) with good enantioselectivity, albeit with significantly diminished yield. Aryl propargyl ethers proved to be excellent substrates, delivering good enantioselectivity while tolerating various substituents on the benzene ring, including *para*-acetyl, *para*-nitro, *para*-trifluoromethyl, *meta*-bromo, and *ortho*-bromo groups, etc (**7a–7j**). Similarly, 2-naphthyl propargyl ether achieved excellent enantioselectivity, though the corresponding product was obtained in only 37% yield (**7k**). Propargyl benzyl ether also demonstrated good compatibility with this coupling system, furnishing **7l** in 49% yield with 98% ee. In contrast, phenylacetylene and *para*-toluenesulfonyl acetylene proved incompatible with this reaction, resulting in either poor enantioselectivity or low yield (**8** and **9**).

Regarding the azide component, the scope remains largely restricted to  $\alpha$ -azido acetate derivatives and benzylic azides.  $\alpha$ -Azido acetates/

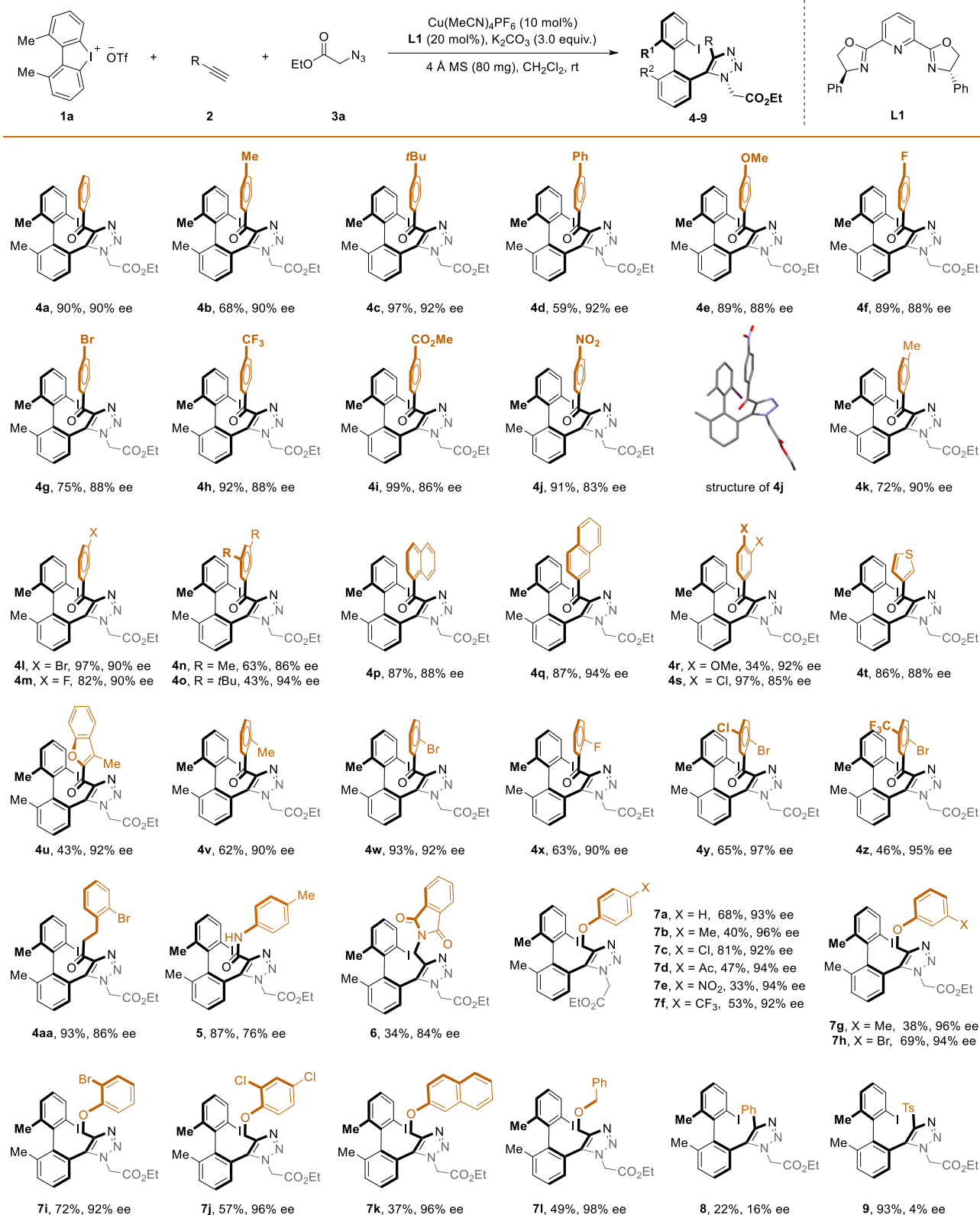


**Fig. 2 | Substrate scope of alkyne.** Conditions: **1** (0.1 mmol), **2** (0.12 mmol), **3** (0.12 mmol),  $\text{Cu}(\text{MeCN})_4\text{PF}_6$  (0.010 mmol), **L1** (0.02 mmol), 4 Å molecular sieves (80 mg),  $\text{K}_2\text{CO}_3$  (3.0 equiv.) in  $\text{CH}_2\text{Cl}_2$  (4 mL), and stirred at 25 °C for 36 h. Isolated yields are reported, and ee values were determined by chiral stationary HPLC.

amides derived from methanol, benzyl alcohols, or benzylamine all furnished good yields and stereoselectivities (**10a**, **10c–10k**), whereas the phenol-based ester exhibited substantially lower efficiency and enantioselectivity (**10b**). Benzylic azides bearing *para*-, *meta*- and *ortho*-

substituents, as well as 2-(azidomethyl)naphthalene, demonstrated good reactivity with enantioselectivity ranging from 76–91% (**10l–10r**). Notably, when  $\text{TsN}_3$  was employed as the substrate, no three-component cross-coupling product **11** was detected. Next, we explored the influence of

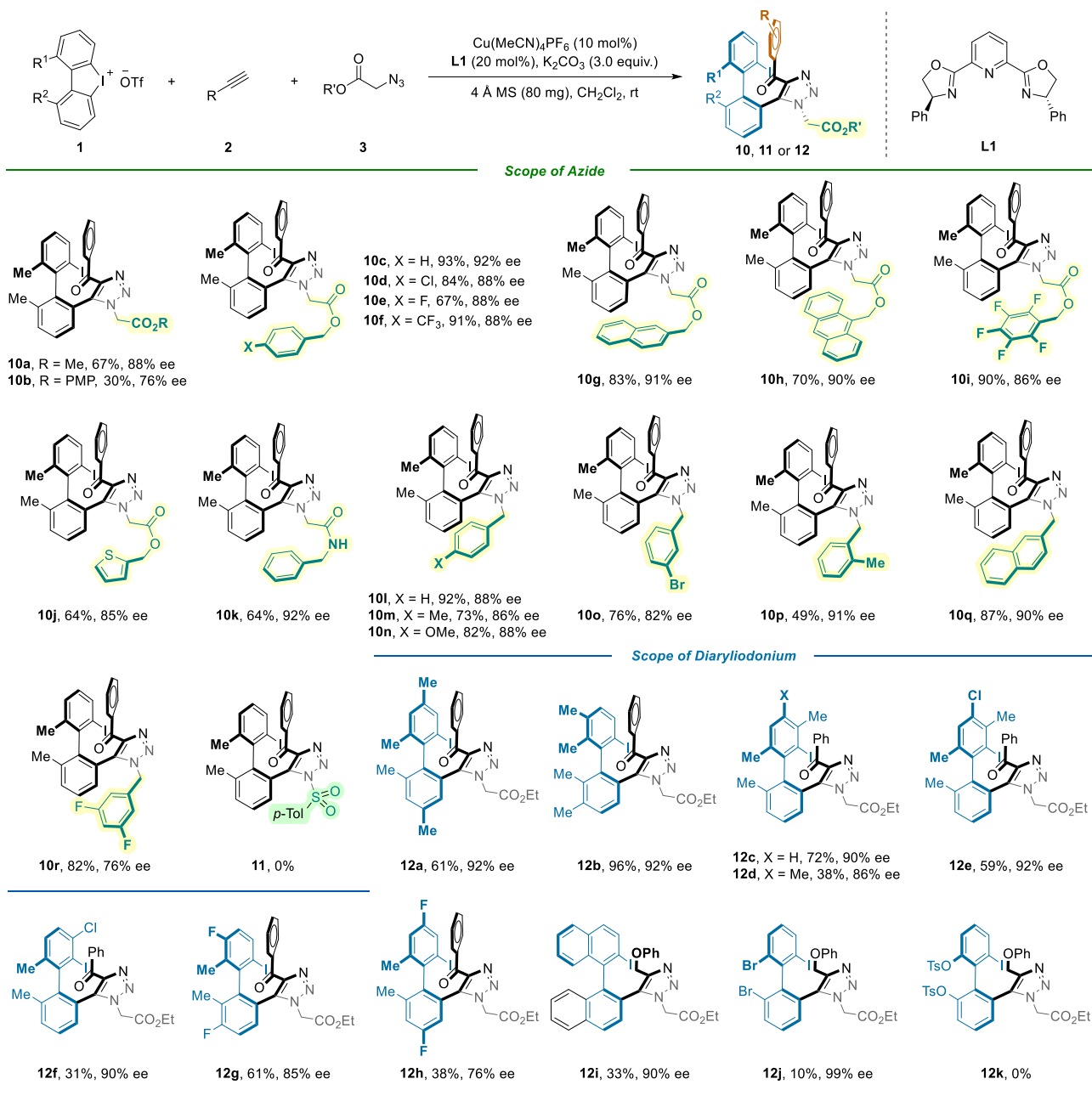


**Fig. 3 | Substrate scope of diaryliodonium and azide.** Conditions: **1** (0.1 mmol), **2** (0.12 mmol), **3** (0.12 mmol), Cu(MeCN)<sub>4</sub>PF<sub>6</sub> (0.010 mmol), **L1** (0.02 mmol), 4 Å molecular sieves (80 mg), K<sub>2</sub>CO<sub>3</sub> (3.0 equiv.) in CH<sub>2</sub>Cl<sub>2</sub> (4 mL), and stirred at 25 °C

for 36 h. Isolated yields are reported, and ee values were determined by chiral stationary HPLC.

various substituents on the cyclic diaryliodonium scaffold. Introducing additional methyl groups at the *meta* or *para* positions relative to the C–I bond maintained good yields and enantioselectivities (**12a** and **12b**). However, with a few exceptions (e.g., **12c** and **12e**), incorporating *ortho*-methyl or chloro group at the C–I bond significantly reduced the yields (**12d** and **12f**). Cyclic diaryliodoniums with fluoro groups at the *meta* or *para* positions relative to the C–I bond resulted in diminished enantioselectivity (**12g** and **12h**). The cross-coupling reactions involving phenyl propargyl ether and  $\alpha$ -azido acetate with binaphthenyl cycloiodonium or 1,9-dibromodibenzoiodonium gave excellent enantioselectivity, albeit with fairly low mass yields (**12i** and **12j**). Finally, 1,9-bis(tosyloxy)dibenzo[*b,d*]iodonium proved ineffective as a substrate, with no desired product being detected (**12k**).

### Mechanistic studies

We subsequently investigated the mechanism of this enantioselective interrupted CuAAC reaction. Alkynyl copper species **2a**-Cu was prepared independently, which can smoothly react cyclic diaryliodonium **1a** to give the alkylation product **13** in moderate yield (Fig. 4a). However, the catalytic reaction between **1a** and **2a** proceeded significantly more slowly than the three-component coupling involving **1a**, **2a**, and **3a**, resulting in the formation of **13** in 22% yield with only 36% enantioselectivity, which contrasted sharply with the high enantioselectivity observed in the three-component reaction (Fig. 4b and 4c). Furthermore, attempted cycloaddition reaction between **13** and azide **3a** under the standard condition failed to proceed. These findings clearly ruled out a mechanism in which the three-

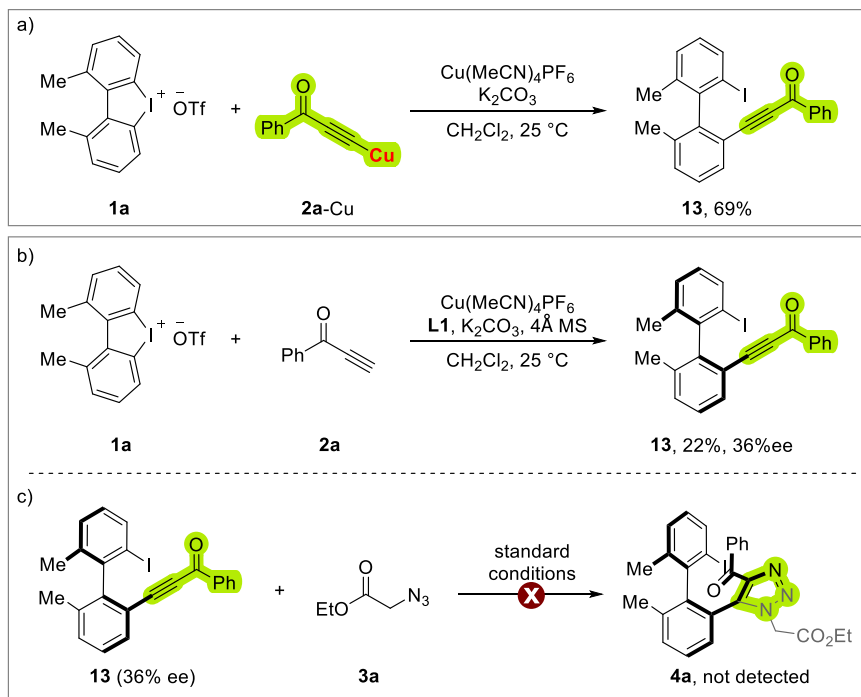


**Fig. 4 | Mechanistic experiments.** **a** The reaction of alkynyl copper **2a-Cu** with cyclic diaryliodonium. **b** Catalytic asymmetric reaction between **1a** and **2a**. **c** Catalytic reaction between **13** and **3a**.

component coupling product was simply aroused from a subsequent [3 + 2] cycloaddition between **13** and **3a**.

Next, we investigated the standard [3 + 2] cycloaddition reaction between **2a** and **3a**, which proved highly sensitive to reaction conditions: in the absence of an additional base and molecular sieves, the reaction proceeded slowly (Fig. 5a). Subsequently, reaction between cyclic diaryliodonium **1a** and triazole **14** was tested under standard conditions, and no final product **4a** was detected, ruling out the possibility of a Cu-catalyzed C-H activation-initiated ring-opening reaction between cyclic diaryliodonium **1a** and compound **14**. Notably,  $\text{K}_2\text{CO}_3$  accelerated the reaction but a dimeric triazole **15** can be detected (Fig. 5b). Replacing alkyne **2a** with the copper acetylide **2a-Cu** in the three-component reaction yielded 20% of **4a** (48% ee), 22% of **13**, along with a small amount of **14** and the dimeric product **15** (Fig. 5c)<sup>57</sup>. These results deviate from the those in Fig. 2, suggesting that **2a-Cu** competes with the copper triazolidine intermediate for oxidative addition with the cyclic diaryliodoniums, and is therefore unlikely to be the active intermediate in the catalytic version employing **1a**, **2a**, and **3a**. Further monitoring by nuclear magnetic resonance (NMR) showed that 4 Å molecular sieves slowed the overall process, and also diminished the byproduct **14** (Fig. 5d, and Supplementary Table S2).

Reaction progress kinetic analysis (RPKA), following the approach introduced by Blackmond et al., was conducted using calorimetric measurements to continuously monitor reactions under synthetically relevant conditions<sup>58–60</sup>. In this three-component reaction, a kinetic isotope effect (KIE) of 0.84 was observed upon using deuterated alkyne **2a-d** in comparison with **2a**, indicating an inverse secondary isotope effect (Fig. 6a, and Supplementary Fig. S2)<sup>61</sup>. This observation implies that the rate-determining step involves changes in the hybridization of the carbon atom attaching hydrogen/deuterium. In contrast, the [3 + 2] cycloaddition between **2a/2a-d** and **3a** exhibited a KIE of 1.44 (Supplementary Fig. S3), suggesting that C–H bond cleavage is likely rate-limiting step under those conditions. These results highlight that using the diaryliodonium reagent to quench the copper triazolidine intermediate fundamentally alters the rate-determining step relative to

a pathway where the copper species is terminated through protonation (Supplementary Figs. S4–S8). Further calorimetric studies evaluating each substrate's impact on the reaction revealed first-order kinetics in both **2a** and **3a** (Fig. 6b). However, a formal 0.4th-order dependence on **1a** was observed, suggesting that the reaction rate is possibly governed by multiple transient intermediates in this multi-step process. Notably, product inhibition prevented complete conversion at low copper catalyst loadings (see below), which complicated detailed kinetic analysis. Nevertheless, similar analysis of the copper catalyst gave a rough conclusion: copper catalyst displayed concentration-dependent behavior. First-order dependence on [Cu] was observed at loadings below 1.0 mol%, but shifted to zeroth-order kinetics when the catalyst loading exceeded 1 mol%.

During our investigation, we found that reducing the copper catalyst loading (e.g., to 2–5 mol%) led to incomplete conversion and a slight decrease in enantioselectivity. We hypothesized that the product or byproducts of this reaction might cause catalyst deactivation or inhibition, or promote the formation of off-cycle copper species, thus reducing the concentration of active copper. To explore this possibility, we added one extra equivalent of product **4a** to the interrupted CuAAC reaction and observed a noticeably slower reaction rate (red curve vs. blue curve in Fig. 7 and Supplementary Fig. S9.). These results suggest that the triazole moiety of **4a** may coordinate to the copper atom, thereby diminishing the  $[\text{Cu}]_{\text{active}}$ .

Based on the above experimental observations and relevant literatures, we propose a possible mechanism for the cyclic diaryliodonium-interrupted CuAAC reaction (Fig. 8). In the two-component CuAAC reaction between benzoylacetylene **2a** and azide **3a**, it is generally accepted that the rate-determining step is the protonation step of triazolyl copper with the alkyne, in line with existing CuAAC kinetic studies (Fig. 8a). In 2013, Fokin et al. extensively investigated the formation of a copper triazolidine intermediate from an alkyne and an azide, identifying a key dinuclear copper species<sup>62,63</sup>. However, in our catalytic system, we suggested that an alkynyl copper intermediate  $\text{RC}\equiv\text{CCu}(\text{I})$  may be not the key intermediate, which is not always necessary for CuAAC reaction (Fig. 8b)<sup>64</sup>. Instead,  $\text{Cu}(\text{I})^*$  may

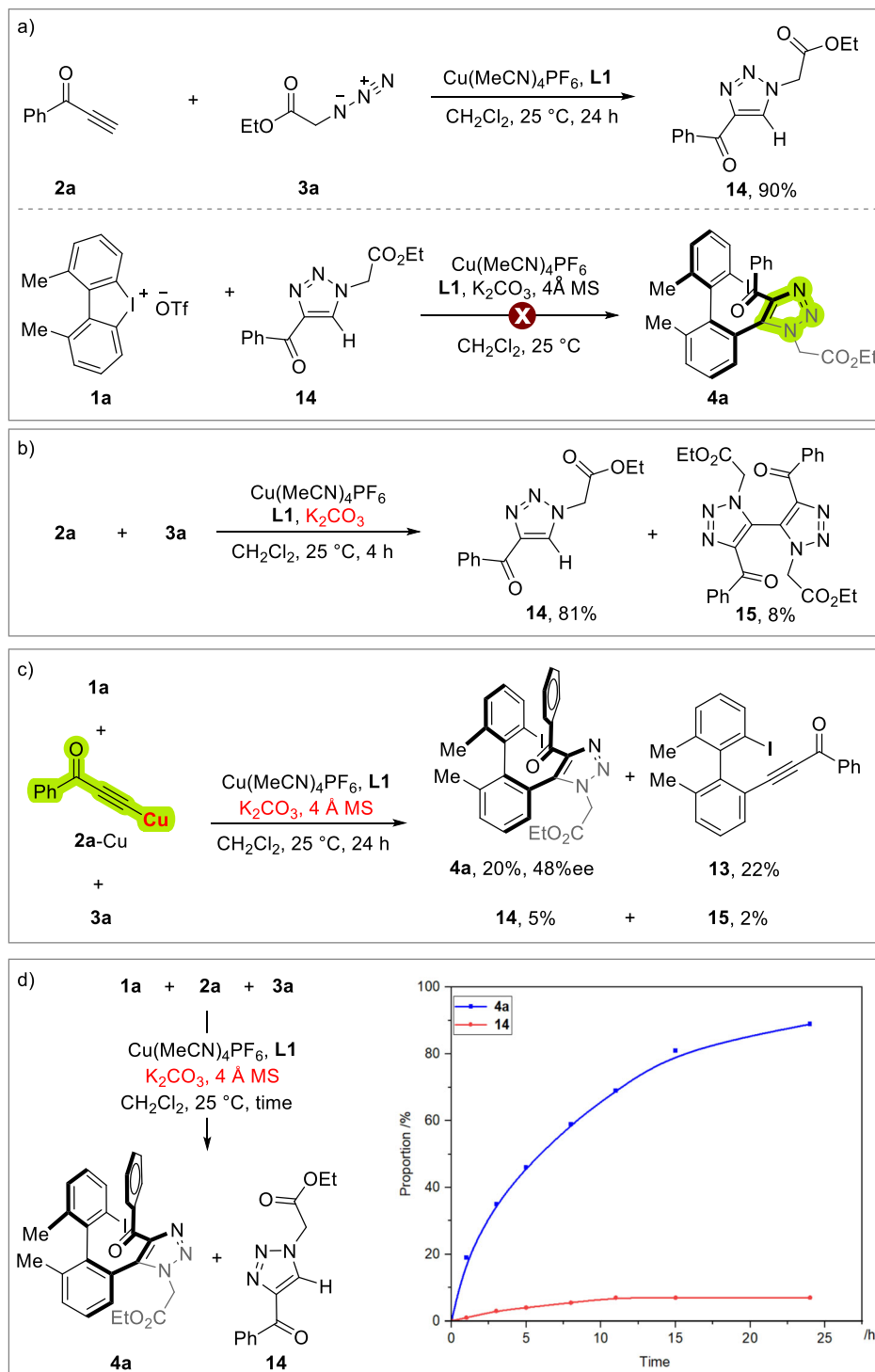


**Fig. 5 | Mechanistic experiments.** **a–b** The effect of  $K_2CO_3$  and attempted cycloaddition between **1a** and **14**. **c** Three-component reaction of **1a**, **3a** and alkynyl copper intermediate **2a-Cu**. **d** Analysis the reaction progress by  $^1H$  NMR.

react both benzoylacetylene and azide in a concerted cyclization to give intermediate **M3**, involving conversion of a  $C(sp)-H$  into a  $C(sp^2)-H$  bond. Under basic conditions, **M3** undergoes an elimination followed by rearrangement, potentially via a vinylidene copper species, to generate **M2**. Next, the cyclic diaryliodonium undergoes oxidative addition with **M2**, furnishing a trivalent copper species **M4** that incorporates an axially chiral framework; this step determines the reaction's stereoselectivity. Finally, reductive elimination from **M4** delivers the product **4a** and regenerates the Cu(I) catalyst. From our kinetic studies, several points merit further explanation: (a) The rate of

copper triazolide quenching by the cyclic diaryliodonium exceeds the protonation rate ( $k_4 > k_3$ ). (b) The rates  $k_1$  and  $k_4$  are likely comparable and collectively influence the overall reaction rate, as evidenced by two observations: (i) an inverse secondary isotope effect for the terminal alkyne C-H bond, and (ii) an apparent 0.4th-order dependence on the cyclic iodonium. (c) The product may coordinate to  $Cu(I)L^*$  in a coordination-dissociation equilibrium, thereby causing product inhibition in the reaction.

In summary, we have developed an asymmetric interrupted CuAAC reaction by capturing the copper triazolide intermediate with cyclic

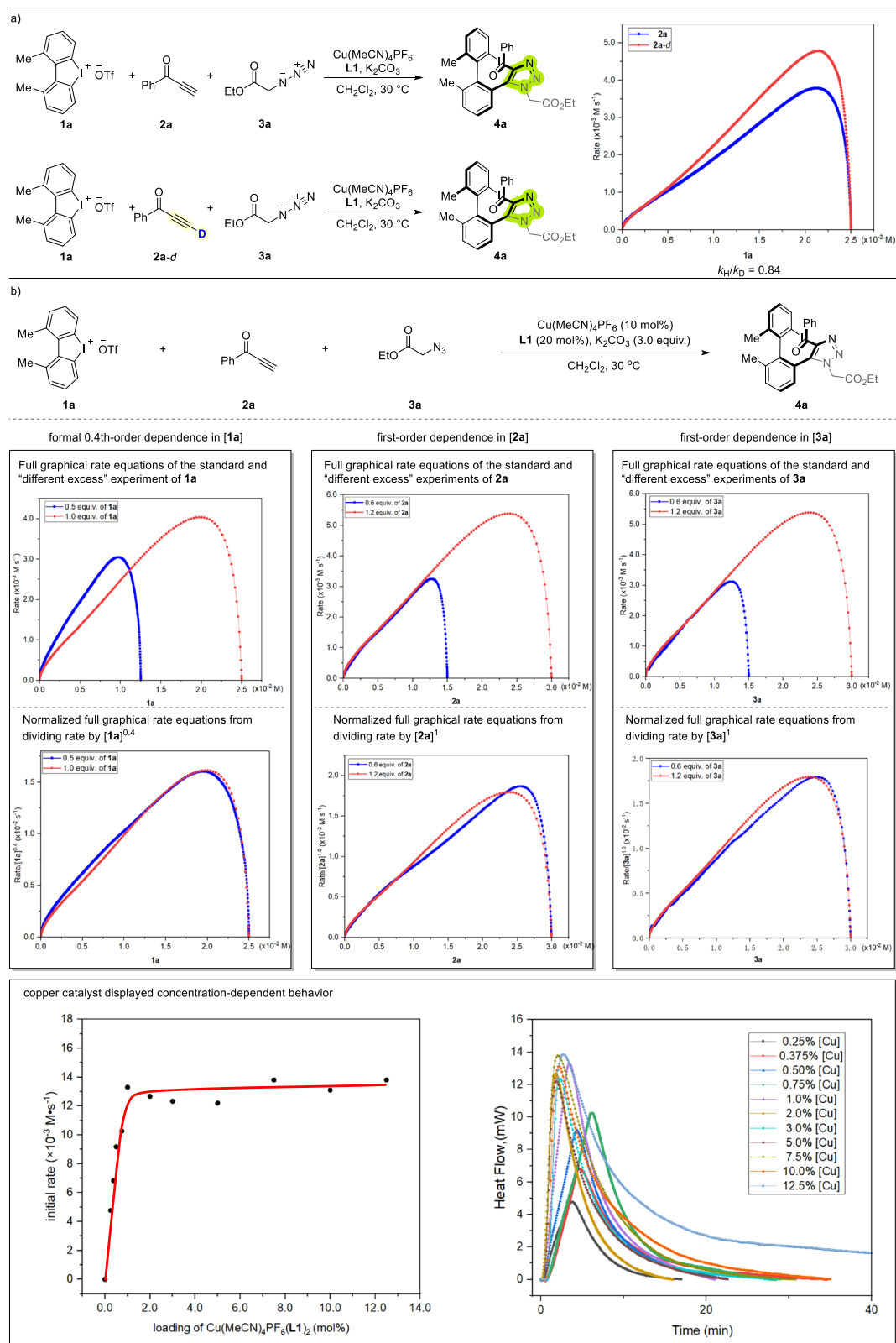


**Fig. 6 | Kinetic studies. a** Kinetic isotope effect analysis with **2a** and **2a-d**. **b** Measuring the orders of three different substrates.

diaryliodoniums, thereby providing an efficient route to a variety of atropisomeric biaryl triazoles and significantly expanding the CuAAC repertoire. Moreover, this work also marks an application of formal carbon nucleophiles in a copper-catalyzed atroposelective ring-opening of cyclic diaryliodoniums for atropisomer synthesis. Mechanistic studies uncovered three key insights: (a) quenching of the copper triazolide

intermediate by the cyclic diaryliodoniums outcompetes the protonation reaction by terminal alkynes<sup>65</sup>; (b) an inverse secondary kinetic isotope effect for the terminal alkyne indicates that the conversion of its terminal carbon center from  $sp$  to  $sp^2$  hybridization is the rate-determining step; and (c) adding extra triazole product to the standard reaction mixture notably diminishes the reaction rate, implying

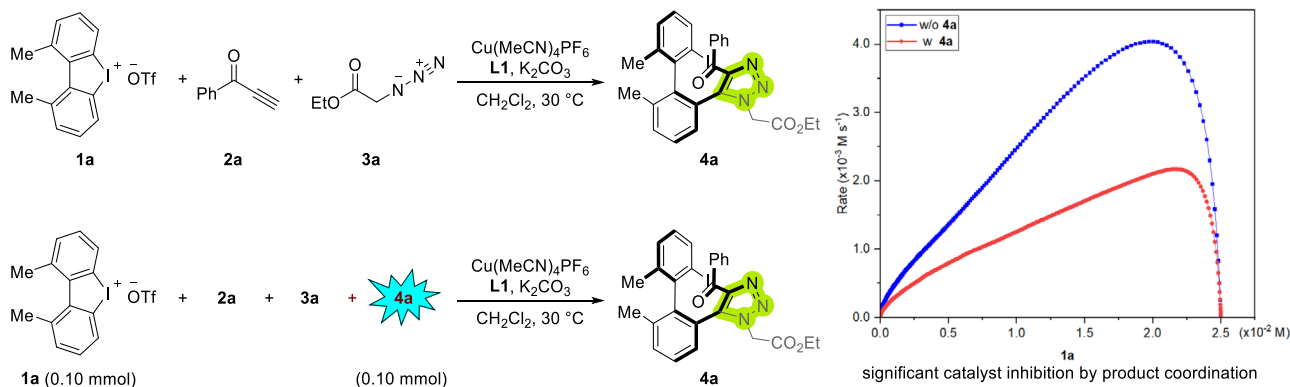


**Fig. 7** | Graphical rate equations of the standard three-component reaction and the reaction with additional product **4a**.

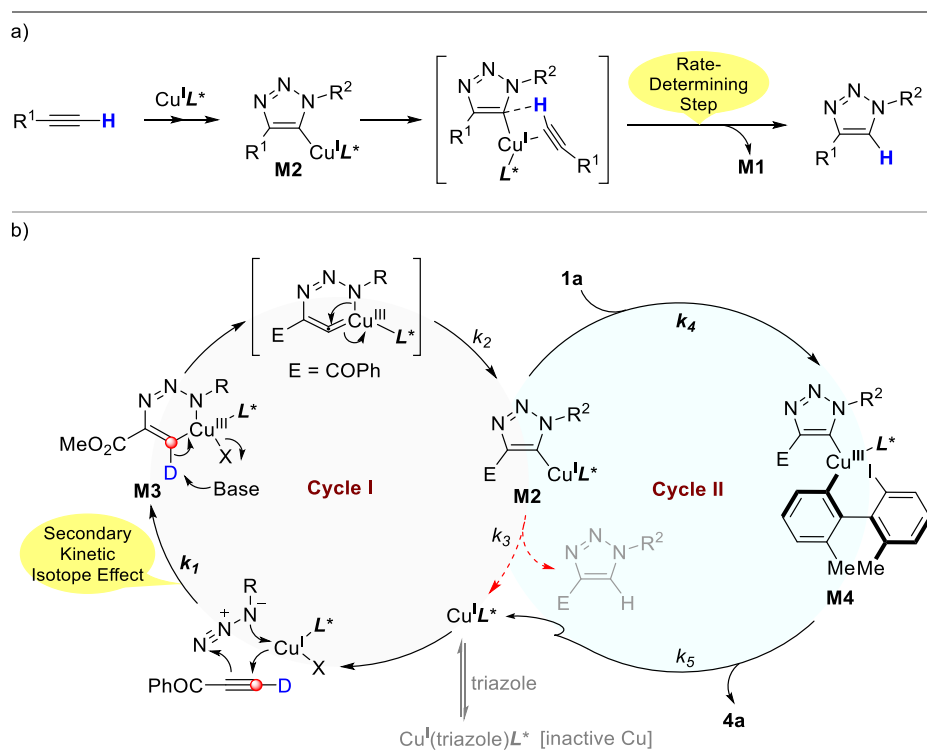


**Fig. 8** | Plausible catalytic cycle. **a** Pathway for Classic CuAAC in Aprotic Solvent. **b** Rationale for Cu-catalyzed Coupling of Alkyne, Azide and Diaryliodonium.

that triazole effectively competes with pyridine-2,6-bis(oxazoline), e.g., **L1**, for copper coordination. Consequently, designing ligands that coordinate more strongly to copper—and thus mitigate triazole's competitive binding—may offer alternative pathways to lower catalyst loadings and enhance stereoselectivity in our future research.

## Method

### General procedure for Cu-catalyzed coupling of cyclic iodonium, propynones, azidoacetates in $\text{CH}_2\text{Cl}_2$

4 Å Molecular sieves (80 mg) in a Schlenk tube were dried by a heating gun under vacuum at 400 °C for 5 min. After cooling down,  $\text{Cu}(\text{MeCN})_4\text{PF}_6$  (3.7 mg, 0.01 mmol, 10 mol%), **L1** (7.4 mg, 0.02 mmol, 20 mol%) and anhydrous  $\text{CH}_2\text{Cl}_2$  (2.0 mL) were added, the resulting mixture was stirred for 30 min. Cyclic diaryliodonium salt **1** (0.10 mmol, 1.0 equiv.), propynone **2** (0.12 mmol, 1.2 equiv.) and azidoacetate **3** (0.12 mmol, 1.2 equiv.) were added. After stirring at 25 °C for 30 seconds, potassium carbonate (41.5 mg, 0.30 mmol, 3.0 equiv.) (pre-dried by a heating gun under vacuum at 400 °C for 3 minutes) and anhydrous

$\text{CH}_2\text{Cl}_2$  (2.0 mL) were added and stirred at 25 °C for 36 h. After complete consumption of diaryliodonium, the mixture was filtered through a plug of celite with ethyl acetate. The filtrate was concentrated under reduced pressure, and the residue was purified by column chromatography on silica gel to deliver the corresponding product.

## Data availability

Deposition Number 2421103 contains the supplementary crystallographic data for this paper. These data can be obtained free of charge via the joint Cambridge Crystallographic Data Center (CCDC) and Fachinformationszentrum Karlsruhe Access Structures service. These data can be obtained free of charge via [www.ccdc.cam.ac.uk/data\\_request/cif](http://www.ccdc.cam.ac.uk/data_request/cif), by emailing [data\\_request@ccdc.cam.ac.uk](mailto:data_request@ccdc.cam.ac.uk), or by contacting The Cambridge Crystallographic Data Center, 12 Union Road, Cambridge CB2 1EZ, UK; fax: + 441223 336033. Data supporting the findings of this manuscript are also available from within the Supplementary Information and from the corresponding author upon request.

## References

- Rostovtsev, V. V., Green, L. G., Fokin, V. V. & Sharpless, K. B. A stepwise Huisgen cycloaddition process: copper(I)-catalyzed regioselective “ligation” of azides and terminal alkynes. *Angew. Chem. Int. Ed.* **41**, 2596–2599 (2002).
- Tornøe, C. W., Christensen, C. & Meldal, M. Peptidotriazoles on solid phase: [1,2,3]-triazoles by regioselective copper(I)-catalyzed 1,3-dipolar cycloadditions of terminal alkynes to azides. *J. Org. Chem.* **67**, 3057–3064 (2002).
- Meldal, M. & Diness, F. Recent fascinating aspects of the CuAAC click reaction. *Trends Chem.* **2**, 569–584 (2020).
- Neumann, S., Biewend, M., Rana, S. & Binder, W. H. The CuAAC: principles, homogeneous and heterogeneous catalysts, and novel developments and applications. *Macromol. Rapid Commun.* **41**, 1900359 (2020).
- Hein, J. E. & Fokin, V. V. Copper-catalyzed azide–alkyne cycloaddition (CuAAC) and beyond: new reactivity of copper(I) acetylides. *Chem. Soc. Rev.* **39**, 1302–1315 (2010).
- Wang, Q. et al. Bioconjugation by Copper(I)-Catalyzed Azide–Alkyne [3 + 2] Cycloaddition. *J. Am. Chem. Soc.* **125**, 3192–3193 (2003).
- Dohler, D., Michael, P. & Binder, W. H. CuAAC-based click chemistry in self-healing polymers. *Acc. Chem. Res.* **50**, 2610–2620 (2017).
- Zhou, F. et al. Asymmetric copper(I)-Catalyzed Azide–Alkyne cycloaddition to quaternary oxindoles. *J. Am. Chem. Soc.* **135**, 10994–10997 (2013).
- Gong, Y. et al. Sulfonyl-PYBOX ligands enable kinetic resolution of  $\alpha$ -tertiary azides by CuAAC. *Angew. Chem. Int. Ed.* **62**, e202301470 (2023).
- Zhu, L., Brassard, C. J., Zhang, Z., Guha, P. M. & Clark, R. J. On the mechanism of Copper(I)-Catalyzed Azide–Alkyne cycloaddition. *Chem. Rec.* **16**, 1501–1517 (2016).
- Nolte, C., Mayer, P. & Straub, B. Isolation of a Copper(I) Triazolide: a “Click” intermediate. *Angew. Chem. Int. Ed.* **46**, 2101–2103 (2007).
- Winn, J., Pinczewska, A. & Goldup, S. M. Synthesis of a rotaxane CuI triazolide under aqueous conditions. *J. Am. Chem. Soc.* **135**, 13318–13321 (2013).
- Wu, Y.-M., Deng, J., Li, Y. & Chen, Q.-Y. Regiospecific synthesis of 1,4,5-trisubstituted-1,2,3-triazole via one-pot reaction promoted by Copper(I) Salt. *Synthesis* **2005**, 1314–1318 (2005).
- Deng, X. et al. Allyl-assisted, Cu(I)-catalyzed azide–alkyne cycloaddition/allylation reaction: assembly of the [1,2,3]Triazol-4,5,6,7-tetrahydropyridine core structure. *J. Org. Chem.* **80**, 11003–11012 (2015).
- Wang, W., Peng, X., Wei, F., Tung, C.-H. & Xu, Z. Copper(I)-catalyzed interrupted click reaction: synthesis of diverse 5-hetero-functionalized triazoles. *Angew. Chem. Int. Ed.* **55**, 649–653 (2016).
- Larin, E. M. & Lautens, M. Intramolecular Copper(I)-catalyzed interrupted click–acylation domino reaction. *Angew. Chem. Int. Ed.* **58**, 13438–13442 (2019).
- Li, L., Zhang, G., Zhu, A. & Zhang, L. A convenient preparation of 5-iodo-1,4-disubstituted-1,2,3-triazole: multicomponent one-pot reaction of Azide and Alkyne mediated by CuI-NBS. *J. Org. Chem.* **73**, 3630–3633 (2008).
- Wang, W., Lin, Y., Ma, Y., Tung, C.-H. & Xu, Z. Copper(I)-catalyzed three-component click/persulfuration cascade: regioselective synthesis of triazole disulfides. *Org. Lett.* **20**, 2956–2959 (2018).
- Wei, F., Zhou, T., Ma, Y., Tung, C.-H. & Xu, Z. Bench-stable 5-stannyl triazoles by a Copper(I)-catalyzed interrupted click reaction: bridge to trifluoromethyltriazoles and trifluoromethylthiotriazoles. *Org. Lett.* **19**, 2098–2101 (2017).
- Teixeira, W. K. O. et al. Copper-mediated intramolecular interrupted CuAAC selenylation. *J. Org. Chem.* **88**, 10434–10447 (2023).
- Pothi, T. A. & Ramana, C. V. Intramolecular nitrene interrupted click reaction. *Org. Lett.* **26**, 2233–2237 (2024).
- Brunelli, F., Russo, C., Giustiniano, M. & Tron, G. C. Each interruption is an opportunity: novel synthetic strategies explored through interrupted click reactions. *Chem. Eur. J.* **30**, e202303844 (2024).
- Wang, W. et al. Copper(I)-catalyzed interrupted click/sulfenylation cascade: one-pot synthesis of sulfur cycle fused 1,2,3-triazoles. *Chin. J. Chem.* **38**, 445–448 (2020).
- Sun, P. et al. Copper(I)-catalyzed multicomponent interrupted click reaction: modular synthesis of triazole sulfides from elemental sulfur. *Org. Chem. Front.* **10**, 1890–1896 (2023).
- Wu, F. et al. Copper mediated three-component reactions of alkynes, azides, and propargylic carbonates: synthesis of 5-allenyl-1,2,3-triazoles. *Adv. Synth. Catal.* **360**, 2435–2439 (2018).
- Cheung, K. P. S. & Tsui, G. C. Copper(I)-Catalyzed interrupted click reaction with TMSCF<sub>3</sub>: synthesis of 5-trifluoromethyl 1,2,3-triazoles. *Org. Lett.* **19**, 2881–2884 (2017).
- Cai, Q., Yan, J. & Ding, K. A CuAAC/Ullmann C-C coupling tandem reaction: copper-catalyzed reactions of organic azides with N-(2-iodoaryl)-propiolamides or 2-iodo-N-(prop-2-ynyl)-benzenamines. *Org. Lett.* **14**, 3332–3335 (2012).
- Reddy, M. N. & Swamy, K. C. K. Facile Construction of [6,6]-, [6,7]-, [6,8]-, and [6,9]ring-fused triazole frameworks by copper-catalyzed, tandem, one-pot, click and intramolecular arylation reactions: elaboration to fused pentacyclic derivatives. *Eur. J. Org. Chem.* **10**, 2013–2022 (2012).
- Pericherla, K., Jha, A., Khungar, B. & Kumar, A. Copper-catalyzed tandem azidealkyne cycloaddition, Ullmann type C-N coupling, and intramolecular direct arylation. *Org. Lett.* **15**, 4304–4307 (2013).
- Liu, Z. et al. Mild Cu(I)-catalyzed cascade reaction of cyclic diaryliodoniums, sodium azide, and alkynes: efficient synthesis of triazolophenanthridines. *Org. Lett.* **16**, 5600–5603 (2014).
- Lanman, B. A., Parsons, A. T. & Zech, S. G. Addressing atropisomerism in the development of sotorasib, a covalent inhibitor of KRAS G12C: structural, analytical, and synthetic considerations. *Acc. Chem. Res.* **55**, 2892–2903 (2022).
- Kozłowski, M. C., Morgan, B. J. & Linton, E. C. Total synthesis of chiral biaryl natural products by asymmetric biaryl coupling. *Chem. Soc. Rev.* **38**, 3193–3207 (2009).
- Bringmann, G., Gulder, T., Gulder, T. A. M. & Breuning, M. Atroposelective total synthesis of axially chiral biaryl natural products. *Chem. Rev.* **111**, 563–639 (2011).
- Perreault, S., Chandrasekhar, J. & Patel, L. Atropisomerism in drug discovery: a medicinal chemistry perspective inspired by atropisomeric class I PI3K inhibitors. *Acc. Chem. Res.* **55**, 2581–2593 (2022).
- Bringmann, G. et al. Atroposelective synthesis of axially chiral biaryl compounds. *Angew. Chem. Int. Ed.* **44**, 5384–5427 (2005).
- Wencel-Delord, J., Panossian, A., Leroux, F. R. & Colobert, F. Recent advances and new concepts for the synthesis of axially stereoenriched biaryls. *Chem. Soc. Rev.* **44**, 3418–3430 (2015).
- Loxq, P., Manoury, E., Pol, R., Deydier, E. & Labande, A. Synthesis of axially chiral biaryl compounds by asymmetric catalytic reactions with transition metals. *Coord. Chem. Rev.* **308**, 131–190 (2016).
- Link, A. & Sparr, C. Stereoselective arene formation. *Chem. Soc. Rev.* **47**, 3804–3815 (2018).
- Carmona, J., Rodríguez-Franco, C., Fernández, R., Hornillos, V. & Lassaletta, J. Atroposelective transformation of axially chiral (hetero)biaryls. From desymmetrization to modern resolution strategies. *Chem. Soc. Rev.* **50**, 2968–2983 (2021).
- Cheng, J. K., Xiang, S.-H., Li, S., Ye, L. & Tan, B. Recent advances in catalytic asymmetric construction of atropisomers. *Chem. Rev.* **121**, 4805–4902 (2021).
- Li, T.-Z., Li, S.-J., Tan, W. & Shi, F. Catalytic asymmetric construction of axially chiral indole-based frameworks: an emerging area. *Chem. Eur. J.* **26**, 15779–15792 (2020).

42. Wu, Y.-J., Liao, G. & Shi, B.-F. Stereoselective construction of atropisomers featuring a C-N chiral axis. *Green Synth. Catal.* **3**, 117–136 (2022).
43. Feng, J., Lu, C.-J. & Liu, R.-R. Catalytic asymmetric synthesis of atropisomers featuring an Aza axis. *Acc. Chem. Res.* **56**, 2537–2554 (2023).
44. Roos, C. B. et al. Stereodynamic strategies to induce and enrich chirality of atropisomers at a late stage. *Chem. Rev.* **123**, 10641–10727 (2023).
45. Choppin, S. & Wencel-Delord, J. Sulfoxide-directed or 3d-metal catalyzed C–H activation and hypervalent iodines as tools for atroposelective synthesis. *Acc. Chem. Res.* **56**, 189–202 (2023).
46. Coquerel, Y. Aryne atropisomers: chiral arynes for the enantioselective synthesis of atropisomers and nanographene atropisomers. *Acc. Chem. Res.* **56**, 86–94 (2023).
47. Portolani, C., Centonze, G., Righi, P. & Bencivenni, G. Role of cinchona alkaloids in the enantio- and diastereoselective synthesis of axially chiral compounds. *Acc. Chem. Res.* **55**, 3551–3571 (2022).
48. Luo, W., Zhang, Y., Ming, M. & Zhang, L. Recent advances in the catalytic asymmetric construction of axially chiral azole-based frameworks. *Org. Chem. Front.* **11**, 6819–6849 (2024).
49. Zhao, K. et al. Enhanced reactivity by torsional strain of cyclic diaryliodonium in Cu-catalyzed enantioselective ring-opening reaction. *Chem* **4**, 599–612 (2018).
50. Zhao, K., Yang, S., Gong, Q., Duan, L. & Gu, Z. Diols activation via Cu/Borinic acids synergistic catalysis in atroposelective ring-opening of cyclic diaryliodoniums. *Angew. Chem. Int. Ed.* **60**, 5788–5793 (2021).
51. Li, Y., Duan, L., Hong, B. & Gu, Z. Preparation of optically active 2,2'-Dibromo-6,6'-diiodo-1,1'-biphenyl: a powerful precursor for modular synthesis of functionalized atropisomers. *Chin. J. Chem.* **41**, 3515–3520 (2023).
52. Kina, A., Miki, H., Cho, Y.-H. & Hayashi, T. Palladium-catalyzed Heck and carbonylation reactions of a dinaphthaleneiodonium salt forming functionalized 2-iodo-1,1'-binaphthyls. *Adv. Synth. Catal.* **346**, 1728–1732 (2004).
53. Han, J. et al. Enantioselective double carbonylation enabled by high-valent palladium catalysis. *J. Am. Chem. Soc.* **144**, 21800–21807 (2022).
54. Zhang, X., Zhao, K. & Gu, Z. Transition metal-catalyzed biaryl atropisomer synthesis via a torsional strain promoted ring-opening reaction. *Acc. Chem. Res.* **55**, 1620–1633 (2022).
55. Özen, C. & Tüzün, N. S. Mechanism of CuAAC reaction: in acetic acid and aprotic conditions. *J. Mol. Catal. A: Chem.* **426**, 150–157 (2017).
56. Brotherton, W. S. et al. Apparent copper(II)-accelerated azide-alkyne cycloaddition. *Org. Lett.* **11**, 4954–4957 (2009).
57. Laborde, C. et al. Double [3+2]-dimerisation cascade synthesis of bis(triazolyl)bisphosphanes, a new scaffold for bidentate bisphosphanes. *Dalton Trans.* **44**, 12539–12545 (2015).
58. Ferretti, A. C., Mathew, J. S. & Blackmond, D. G. Reaction calorimetry as a tool for understanding reaction mechanisms: application to Pd-catalyzed reactions. *Ind. Eng. Chem. Res.* **46**, 8584–8589 (2007).
59. Burés, J., Armstrong, A. & Blackmond, D. G. Explaining anomalies in enamine catalysis: “downstream species” as a new paradigm for stereocontrol. *Acc. Chem. Res.* **49**, 214–222 (2016).
60. Sung, S. et al. Mechanistic studies on the copper-catalyzed N-arylation of alkylamines promoted by organic soluble ionic bases. *ACS Catal.* **6**, 3965–3974 (2016).
61. Gómez-Gallego, M. & Sierra, M. A. Kinetic isotope effects in the study of organometallic reaction mechanisms. *Chem. Rev.* **111**, 4857–4963 (2011).
62. Worrell, B. T., Malik, J. A. & Fokin, V. V. Direct evidence of a dinuclear copper intermediate in Cu(I)-catalyzed azide-alkyne cycloadditions. *Science* **340**, 457–460 (2013).
63. Héron, J. & Balcells, D. Concerted cycloaddition mechanism in the CuAAC reaction catalyzed by 1,8-naphthyridine dicopper complexes. *ACS Catal.* **12**, 4744–4753 (2022).
64. Fang, Y. et al. Insight into the mechanism of the CuAAC reaction by capturing the crucial Au<sub>4</sub>Cu<sub>4</sub>-π-Alkyne Intermediate. *J. Am. Chem. Soc.* **143**, 1768–1772 (2021).
65. Seath, C. P., Burley, G. A. & Watson, A. J. B. Determining the origin of rate-independent chemoselectivity in CuAAC reactions: an alkyne-specific shift in rate-determining step. *Angew. Chem. Int. Ed.* **56**, 3314–3318 (2017).

## Acknowledgements

The authors are grateful for financial support from the National Key Research and Development Program of China (no. 2021YFA1500100), the National Natural Science Foundation of China (22301291, 22471254), and Open Research Fund of State Key Laboratory of Coordination Chemistry, School of Chemistry and Chemical Engineering, Nanjing University. We also thank the robotic AI-Scientist platform of Chinese Academy of Sciences for conducting substrate-compatibility testing with its chemical robot and for financial support.

## Author contributions

Y.L. and S.Y. conceived the idea, and performed the experiments and characterization of compounds. Z.G. and Y.L. co-wrote the manuscript. Z.G. and L.D. directed the project.

## Competing interests

The authors declare no competing interests.

## Additional information

**Supplementary information** The online version contains supplementary material available at <https://doi.org/10.1038/s41467-026-68574-2>.

**Correspondence** and requests for materials should be addressed to Zhenhua Gu.

**Peer review information** *Nature Communications* thanks Jian Liao, Ricardo Schwab and the other, anonymous, reviewer(s) for their contribution to the peer review of this work. A peer review file is available.

**Reprints and permissions information** is available at <http://www.nature.com/reprints>

**Publisher's note** Springer Nature remains neutral with regard to jurisdictional claims in published maps and institutional affiliations.

**Open Access** This article is licensed under a Creative Commons Attribution-NonCommercial-NoDerivatives 4.0 International License, which permits any non-commercial use, sharing, distribution and reproduction in any medium or format, as long as you give appropriate credit to the original author(s) and the source, provide a link to the Creative Commons licence, and indicate if you modified the licensed material. You do not have permission under this licence to share adapted material derived from this article or parts of it. The images or other third party material in this article are included in the article's Creative Commons licence, unless indicated otherwise in a credit line to the material. If material is not included in the article's Creative Commons licence and your intended use is not permitted by statutory regulation or exceeds the permitted use, you will need to obtain permission directly from the copyright holder. To view a copy of this licence, visit <http://creativecommons.org/licenses/by-nc-nd/4.0/>.

© The Author(s) 2026